JOURNAL OF
Materials
CHEMISTRY

Microwave assisted rapid crystallization of Mg–M(III) hydrotalcite where M(III) = Al, Fe or Cr

Srinivasan Kannan* and Raksh Vir Jasra

Central Salt and Marine Chemicals Research Institute, GB Marg, Bhavnagar 364 002, India.
E-mail: salt@bhavnagar.com

Received 26th May 2000, Accepted 14th July 2000
First published as an Advanced Article on the web 18th August 2000

MgM(III)–carbonate hydrotalcites where M(III) = Al, Fe and Cr were rapidly synthesized through an instantaneous addition method coupled with microwave irradiation. The materials were characterized by powder X-ray diffraction (XRD), thermogravimetric analysis, ^{27}Al MAS-NMR spectroscopy, transmission electron microscopy (TEM) and BET specific surface area measurements. Microwave irradiation resulted in a well crystallized material after a short synthesis time (12 min) compared to conventional coprecipitation and aging of the gel (25.5 h). However, the extent of enhancement in crystallinity upon irradiation depended on the nature of the trivalent metal ion. For the Mg–Cr system, microwave irradiation enhanced the crystallinity of the desired hydrotalcite-like phase at the expense of the impurity brucite phase, while the opposite effect was observed with conventional aging. The charged nature of the hydrotalcite network and water molecules present in the interlayer space enables uniform and effective absorption of microwaves, favoring long range ordering.

Introduction

Hydrotalcite-like compounds, a new class of layered materials having the general molecular formula $[\mathrm{M(II)}_{1-x}\mathrm{M(III)}_x(\mathrm{OH})_2][\mathrm{A}_{x/n}{}^{n-}]\cdot m\mathrm{H_2O}$ (where M(II) and M(III) are divalent and trivalent cations and A is the interlayer anion), have been receiving increasing attention in recent years, owing to their potential applications as catalysts, supports, ion-exchangers and precursor for composite materials.[1–4] Structurally, they possess brucite-like ($Mg(OH)_2$) sheets wherein isomorphous substitution of Mg^{2+} by a trivalent cation, like Al^{3+}, occurs. The resulting excess positive charge of the layered network is compensated by anions, which occupy the interlayer space along with water molecules. Conventionally, these compounds are synthesized by a coprecipitation technique wherein metal nitrates and precipitants are added slowly and simultaneously at a fixed pH under stirring, followed by aging and/or hydrothermal treatments in order to improve the crystallinity.[5] Good crystallinity with tunable textural properties of hydrotalcites is essential for them to be utilized as additives in various catalytic and polymer formulations.[1] The synthesis of a well crystalline hydrotalcite may require a few hours or days depending on the synthetic methodology and nature of the post synthesis treatments.[5,6] Our recent work regarding the influence of various synthetic methodologies on the crystallinity of the aged hydrotalcites (at 338 K for 24 h) showed that the instantaneous addition method gives material with higher crystallinity.[7] In this method, both metal nitrates and precipitants are added in a very short time ($<$5–10 s), in contrast to the coprecipitation method which takes a few hours ($\sim$2–4 h).

Application of microwave irradiation has been reported for the rapid synthesis of inorganic solids and organic synthetic reactions.[8,9] Although the utility of microwaves is emphasized mainly in solid state synthesis, the extension of its application to liquid media has been of recent interest. A well crystallized hydroxyapatite, a hydroxyphosphate of calcium, was synthesized by the microwave method in less than 25 min in contrast to the longer synthetic precipitation or hydrothermal process.[10] The fast reaction is attributed to the microwave coupling of water bound to Ca^{2+} ions in a hydration sheath. Crystallization rate enhancement using microwaves has also been reported for hydrated systems and pillared clays.[11,12] Very recently microwave heating has been utilized in the synthesis of large pore zeolites and aluminium phosphates (AlPOs).[13,14] Gel crystallization of cloverite, a large pore phosphate, has been found to decrease from 1–2 days for the conventional hydrothermal technique to 20 min with the use of microwaves.[13] In the present paper, we report a new methodology for the rapid synthesis of well crystallized MgM(III) hydrotalcites, where M(III) = Al, Fe and Cr, through an instantaneous addition method coupled with microwave heating.

Experimental

Synthesis

Analar grade magnesium nitrate and trivalent metal nitrates (s.d.fine chem., India) were used as the sources of Mg and M(III) while sodium hydroxide and sodium carbonate were procured from Qualigens, India. Solution A, comprising 75 ml of 1 M magnesium nitrate and 25 ml of 1 M M(III) nitrate, and solution B, containing NaOH (0.2 M) and Na_2CO_3 (0.02 M) in 100 ml water, were added instantaneously (less than 5 seconds) to 100 ml of stirring distilled water at ambient temperature (303 K). The obtained gel-like slurry was stirred for 2 min and subjected to microwave treatment. Trial experiments were carried out to optimize the resulting slurry pH at around 10.0. A portion of the fresh gel was aged at 338 K for 24 h without stirring, a time optimized on the basis of previous experiments for obtaining a well crystallized material.[7]

Microwave irradiation was performed over the fresh gel in a conventional domestic oven (800 W with 50% power output; 2.45 GHz). Reactions were performed using 50 ml of gel in a 1 L conical flask for 2.5–10 min. It was noted that at 2.5 min, there was no significant loss of water from the reaction mixture, at 5.0 min a reduction in the volume of water of about one half was observed, and at 10 min a nearly dry sample (more than 95% loss of water) was obtained. In the subsequent discussion, the following terminology is used: MgM(III)-Fresh, Mg M(III)-Aged and MgM(III)-MW*x* to indicate fresh, aged and microwave treated samples wherein *x* stands for the treatment time. All samples were filtered, washed thoroughly with distilled water and dried in an air oven at 383 K overnight.

DOI: 10.1039/b004219f

Characterization methods

Powder X-ray diffraction (PXRD) data were recorded and processed (using PC-APD software) using a Philips X'Pert MPD system using CuKα radiation ($\lambda = 1.5406$ Å). A step size of 0.14° and a step time of 5.6 s were used for data collection. The X-ray beam voltage was 40 kV and beam current was 55 mA. The Debye–Scherrer equation was employed for calculation of the crystallite size after taking into consideration the instrumental line broadening.

FT-IR spectra of these samples were recorded using a Perkin-Elmer spectrometer (Model-Spectrum GX) in the form of KBr discs. The samples were scanned in the region of 4000–400 cm^{-1} with a resolution of less than 2 cm^{-1}.

Thermogravimetric-differential scanning calorimetric (TG-DSC) analyses were performed using a Perkin-Elmer thermal analyzer (TG-DSC-7) in the temperature range 50–850 °C for TG analysis and 50–550 °C for DSC analysis with a heating rate of 10 °C min^{-1} under a nitrogen atmosphere using a 10–15 mg sample. Base line corrections using standards were made prior to analysis of the samples.

Transmission electron microscopy (TEM) of these samples was performed using a JEOL electron microscope (Model 200CX) with an operating voltage of 200 kV. The samples were dispersed in hexane and a drop of supernatant suspension was poured on to a carbon coated copper grid and dried before measurements. Scanning was performed on different regions of the samples to confirm homogeneity.

^{27}Al MAS-NMR spectra of the samples were recorded at 52.15 MHz in a Bruker (Avance DPX 200) NMR spectrometer using 1 M aluminium nitrate solution as an internal standard. The samples were spun at 3000 rpm and spectra were recorded at room temperature.

BET surface areas of the samples were measured in a Flow Sorb II 2300 sorptometer (Micromeritics, USA) using the single point method. Samples were degassed at 150 °C for 2 h prior to measurements.

Results and discussion

Mg–Al system

Elemental analysis of these samples showed (Table 1) no significant difference between input and output Mg/Al atomic compositions, indicating the completion of precipitation. Irrespective of the post synthesis treatment, PXRD patterns of the fresh, aged and microwave irradiated samples showed a pure HT-like phase. Fig. 1(A) and (B) show the (006), and (110) and (113) reflections of fresh, aged and microwave treated samples. It is quite clear that both aging and microwave coupling enhanced the crystallinity of the sample. However, the crystallinity of MgAl-MW10 was higher, considering basal reflections, and comparable, considering *ab* plane reflections, to that of the aged sample. It should be noted here that the synthesis using microwaves took only 12 min while the conventional aging method took 25.5 h. Moreover, the crystallinity of the sample increased with an increase in the microwave heating time. To corroborate the above observation, the crystallite sizes of these samples were measured by the X-ray line broadening technique using the Debye–Sherrer equation ($t = 0.89\lambda/\beta\cos\theta$, where t is the crystallite size, β is the FWHM and θ is the diffraction angle). The basal reflections, namely the (003) and (006) planes, were considered for these measurements and the values are summarized in Table 1. Indeed, a progressive increase in crystallite size with increasing microwave treatment time, indicating an enhancement in long range ordering, was observed while the crystallite sizes for aged and MgAl-MW10 were almost similar. Table 1 summarizes the unit cell parameters of the samples calculated using a least squares fitting method; these were not significantly altered by the employment of different post synthesis treatments. N_2 BET measurements of these samples showed a decrease in specific surface area with an increase in microwave treatment time, with the aged sample showing the highest specific surface area. The higher value for the aged sample could be due to augmented formation and growth of mesopores, which normally contribute to >70% of the total surface area in hydrotalcites.[15]

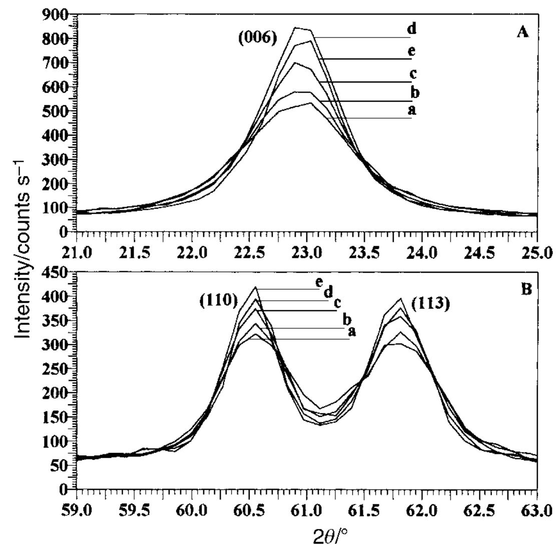

Fig. 1 Effect of post treatment on the intensities of the (A) (006) and (B) (110) and (113) XRD reflections; (a) MgAl-Fresh, (b) MgAl-MW2.5, (c) MgAl-MW5.0, (d) MgAl-MW-10, (e) MgAl-Aged.

To substantiate this crystallinity variation, ^{27}Al MAS-NMR studies were carried out. Fig. 2 shows the ^{27}Al MAS-NMR spectra of some of the samples synthesized. All samples showed a single sharp peak with δ close to 6 ppm indicating the presence of octahedral aluminium.[16] The orderliness of the layer can be elucidated from the asymmetric line broadening which occurs due to the electric field gradient arising from distortion in the octahedral arrangement of the coordinating atoms. This can be evidenced by measuring the full width at half maximum (FWHM), and is more obvous when considering the full width at one-tenth height (FWOTH) of the peaks, the values of which are summarized in Table 1. It is clear from

Table 1 Elemental composition, unit cell parameters, crystallite size, surface area and ^{27}Al MAS-NMR FWOTH of some of the samples synthesized

Sample	Mg/Al atomic ratio	Unit cell parameters/Å		Crystallite size/Å	Surface area/m^2 g^{-1}	FWOTH^a/Hz
		a	*c*			
MgAl-Fresh	3.0	3.057	23.202	89	73	751
MgAl-MW2.5	3.0	3.057	23.257	100	132	
MgAl-MW5.0	3.0	3.057	23.242	116	130	719
MgAl-MW7.5	3.0	3.058	23.267	125	120	
MgAl-MW10.0	3.1	3.056	23.217	140	109	713
MgAl-Aged	3.1	3.058	23.212	150	155	678

^{a}Full width at one-tenth height of ^{27}Al MAS-NMR peak.

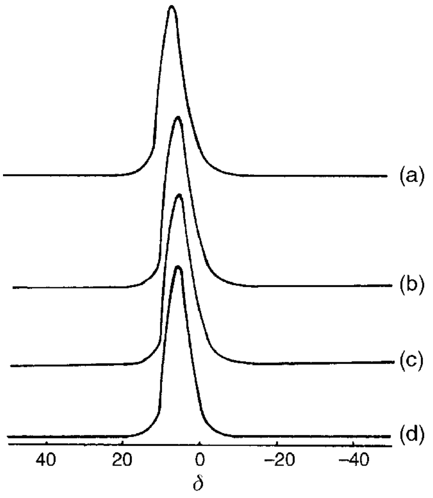

Fig. 2 ^{27}Al MAS-NMR patterns of (a) MgAl-Fresh, (b) MgAl-MW5.0, (c) MgAl-MW10, (d) MgAl-Aged.

these data that the broadening decreased with increasing microwave irradiation time; the broadening is least for the aged samples (*cf*: XRD results).

FT-IR spectra of the samples showed bands around 3500, 1640 and 1370 cm^{-1} which are attributed to ν_{OH} stretching, bending vibrations of water molecules in the interlayer space and ν_3 asymmetric stretching of carbonate. A shift in the position of the ν_{OH} vibration from the free hydroxyl position (3700 cm^{-1}) is due to extensive hydrogen bonding between the layer and the interlayer species. No significant difference in the FT-IR spectra was observed between fresh, aged and microwave treated samples, indicating the uniformity of their layer–interlayer interactions. The bands observed below 1000 cm^{-1} are ascribed to ν_2 and ν_4 vibrations of carbonate, M–(OH) stretching and M–(OH)–M bending vibrations (M = M(II) and/or M(III)).

TEM images of these materials, shown in Fig. 3, exhibit a spherical to hexagonal morphology characteristic of HT-like materials.[15] However, the particle–particle interactions are strong, leading to agglomeration, especially for the fresh samples. Although no noticeable change in the morphology of the samples was observed when different preparation methodologies were used, subtle differences were observed in the morphologies of aged and microwave treated samples, wherein the former showed a spherical to platy morphology while the latter showed a nearly hexagonal morphology.

Thermogravimetric analysis of these samples (Fig. 4) showed a two stage weight loss pattern. The first weight loss is attributed to the removal of water molecules from the interlamellar space while the second weight loss is due to the removal of water through dehydroxylation of sheets and decarbonation of carbonate anion. TG transformation temperatures and the weight losses of some of the samples are given in Table 2. The second weight loss for both the aged and microwave treated samples occurred in a broader temperature window with a weak shoulder around 350 °C, indicating the presence of varied electrostatic interactions prevailing between layered sheets and interlayer molecules. However, on the basis of the transformation temperature (T_2), the microwave irradiated sample showed poor thermal stability while the highest stability was observed for the fresh sample. Further, a continuous weight loss was observed even up to 800 °C. This could be due to the presence of some strongly held carbonate ions, probably with MgAlO solid solutions formed during the heating process.

An interesting observation was noted for the first weight loss pattern of these samples. Dehydration of intercalated water molecules occurred in a wide temperature interval for the fresh and aged samples, and in a sharper temperature interval for microwave treated samples, as clearly seen from the DTG

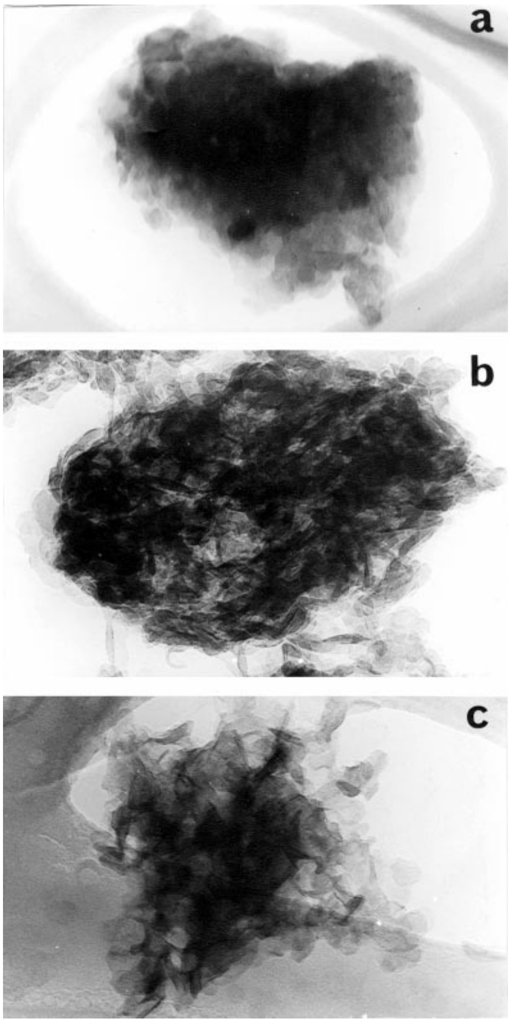

Fig. 3 TEM images of (a) MgAl-Fresh, (b) MgAl-Aged, (c) MgAl-MW10 (1 mm = 60 Å).

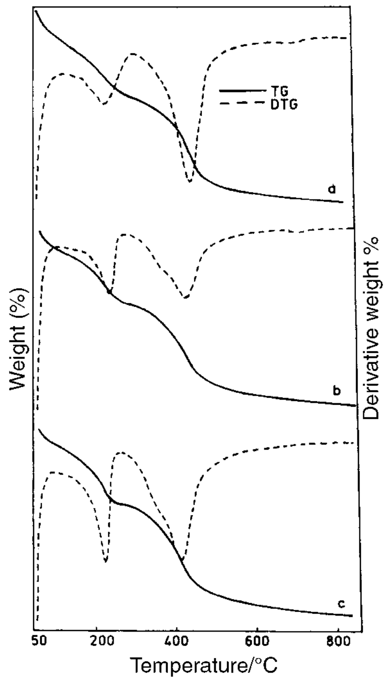

Fig. 4 TG-DTG patterns of (a) MgAl-Fresh, (b) MgAl-Aged, (c) MgAl-MW10.

Table 2 TG transformation temperatures and weight losses observed for some of the samples synthesized

	TG transformation temperature/°C		Weight loss (%)		
Sample	T_1	T_2	First	Second	Net
MgAl-Fresh	224	438	9.8	22.7	48.1
MgAl-Aged	225	361, 414	8.8	22.8	46.0
MgAl-MW10	221	355, 410	10.9	25.3	45.5

traces (Fig. 4). This suggests that microwave coupling results in a better and oriented ordering of water molecules in the interlayer space, unlike conventionally synthesized samples. Such an enhancement in ordering leads to the accommodation of additional water molecules in the interlayer space (Table 2). DSC results substantiated the TG results exhibiting two endotherms for the two stages of weight loss.

Mg–Fe and Mg–Cr systems

We wanted to explore the effectiveness of microwave coupling to more difficult systems and have chosen here the Mg–Fe and Mg–Cr systems. PXRD results showed that microwave coupling enhanced the crystallinity of these samples in shorter times. However, the extent of enhancement in crystallinity depended on the nature of the trivalent metal ion: Cr showed the maximum enhancement followed by Al and Fe respectively. Fig. 5 shows the powder XRD patterns of fresh, aged and microwave (treated for 10 min) irradiated samples of the Mg–Cr system. A fresh sample from this system (Fig. 5a) showed a poorly crystalline HT-like phase along with brucite ($Mg(OH)_2$), an impurity phase. Extended aging of the fresh gel enhanced the crystallinity of the impurity phase to a greater extent. However, microwave irradiation of the fresh gel enhanced the crystallinity of the desired HT-like phase, as clearly evidenced by the development of the (003) and (006) reflections (Fig. 5c), at the expense of the crystallinity of the impurity phase. In other words, a faster rate of crystallization assists in the development of the desired phase for the Mg–Cr system. Such phase transformation of a gel depending on the contact time with the mother liquor is already known in hydrotalcite synthesis, especially for Cu-containing hydrotalcites.[17]

Although the mechanism of interaction of microwaves with materials, especially in liquid media, is unclear, it is proposed that thermal effects along with the nature of material plays a crucial role in enhancing the crystallization rate.[8] We believe here that microwave coupling is effective because of two reasons, namely the charged nature of the hydrotalcite network and the presence of water molecules in the interlayer space (through rotational excitation). This effective interaction facilitates long range ordering in the system in a shorter time. Mingos and coworkers[18] have demonstrated a similar effect while intercalating pyridine and its derivatives in hydrated vanadylphosphate. They attributed the rapid long-range ordering to an autocatalytic effect, which is a consequence of better microwave coupling with the intercalated product.

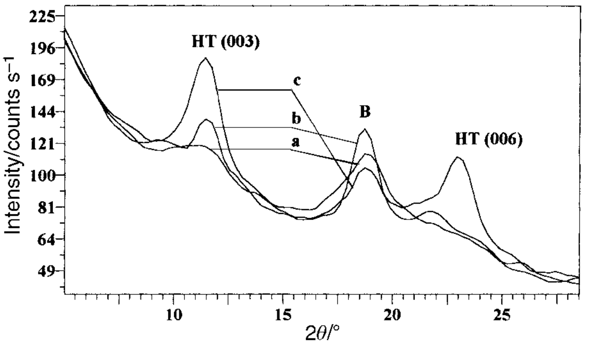

Fig. 5 Powder XRD patterns of (a) MgCr-Fresh, (b) MgCr-Aged, (c) MgCr-MW10 (HT = hydrotalcite; B = brucite).

Conclusions

Microwave irradiation of gels obtained through an instantaneous addition method rapidly enhanced crystallinity. A well crystallized material was obtained in 12 min, in comparison to 1530 min for a conventionally synthesized sample. No significant difference in morphology was observed for microwave treated samples, although subtle variations were noted. Thermal analysis of the Mg–Al system showed that, although weight loss occurred in a wider temperature range, a microwave treated sample possessed lower thermal stability compared to fresh and aged samples. Further, microwave coupling resulted in better and oriented ordering of water molecules in the interlayer space, leading to the accommodation of additional water molecules. The extent of enhancement of the crystallization rate upon irradiation was influenced by the nature of the trivalent cation present in the HT-like network. Rapid crystallization of the Mg–Cr system through microwave irradiation enhanced the crystallinity of the HT-like phase at the expense of the impurity phase. The bipolar nature of these materials and the water present in the interlayer space promote microwave interaction thereby enhancing the rate of crystallization. Efforts are underway to employ microwave irradiation in the synthesis of hydrotalcites, which are difficult to prepare through conventional methods

Acknowledgements

S. K. thanks the Department of Science and Technology for financial assistance under the Young Scientist Scheme. The authors also thank Dr. P. S. Subramanian and Dr. S. Muthusamy for recording MAS-NMR spectra.

References

1 F. Trifiro and A. Vaccari, in *Comprehensive Supramolecular Chemistry, Vol.7, Solid State Supramolecular Chemistry: Two and Three-dimensional Inorganic Networks*, ed. J. L. Atwood, J. E. D. Davies, D. D. MacNicol, F. Vogtle, J-M. Lehn, G. Aberti and T. Bein, Pergamon, Oxford, 1996, p. 251.
2 *Recent Catalytic Applications of Hydrotalcite-type anionic clays*, ed. D. Tichit and A. Vaccari, *Appl. Clay Sci.*, 1998, **13**, 311.
3 V. Rives and M. A. Ulibarri, *Coord. Chem. Rev.*, 1999, **181**, 67.
4 L. M. Parker, N. B. Milestone and R. H. Newmann, *Ind. Eng. Chem. Res.*, 1995, **34**, 1196.
5 A. de Roy, C. Forano, K. El Malki and J-P. Besse, in *Synthesis of Microporous Materials, Vol.2, Expanded Clays and Other Microporous Systems*, ed. M. L. Occelli and H. E. Robson, Van Nostrand Reinhold, New York, 1992, p. 108.
6 S. Kannan and C. S. Swamy, *J. Mater. Sci.*, 1997, **32**, 1623.
7 S. Kannan, *Bull. Catal. Soc. India*, 1999, **9**, 100.
8 K. J. Rao, B. Vaidhyanathan, M. Ganguli and P. A. Ramakrishnan, *Chem. Mater.*, 1999, **11**, 882.
9 D. M. P. Mingos and D. R. Baghurst, *Chem. Soc. Rev.*, 1991, **20**, 1.
10 P. A. Vaidhyanathan and K. J. Rao, *Bull. Mater. Sci.*, 1996, **19**, 1163.
11 S. L. Suib, E. Vileno, Q. Zhang, C. Marun and L. D. Conde, *J. Ceram. Trans.*, 1997, **80**, 331.
12 G. Fetter, G. Heredia, A. M. Maubert and P. Bosch, *J. Mater. Chem.*, 1996, **6**, 1857.
13 H. Kosslick, H. L. Zutowa, U. Lohse, H. Landmesser, R. Fricke and J. Caro, *J. Ceram. Trans.*, 1997, **80**, 523.
14 T. Kodaira, K. Miyazawa, T. Ikeda and Y. Kiyozumi, *Microporous Mesoporous Mater.*, 1999, **29**, 329.
15 W. T. Reichle, S. Y. Kang and D. S. Everhardt, *J. Catal.*, 1986, **101**, 352.
16 M. J. Hudson, S. Carlino and D. C. Apperley, *J. Mater. Chem.*, 1995, **5**, 323.
17 A. Alejandre, F. Medina, P. Salagre, X. Correig and J. E. Sueiras, *Chem. Mater.*, 1999, **11**, 939.
18 K. Chatakondu, M. L. H. Green, D. M. P. Mingos and S. M. Reynolds, *J. Chem. Soc., Chem. Commun.*, 1989, 1515.